Tuning a Bacterial Chemoreceptor with Protein−Membrane Interactions†

Roger R. Draheim, Arjan F. Bormans,‡ Run-Zhi Lai, and Michael D. Manson*

Department of Biology, 3258 TAMU, Texas A&M University, College Station, Texas 77843

Received June 23, 2006; Revised Manuscript Received October 4, 2006

ABSTRACT: Chemoreceptors in *Escherichia coli* are homodimeric transmembrane proteins that convert environmental stimuli into intracellular signals controlling flagellar motion. Chemoeffectors bind to the extracellular (periplasmic) domain of the receptors, whereas their cytoplasmic domain mediates signaling and adaptation. The second transmembrane helix (TM2) connects these two domains. TM2 contains an aliphatic core flanked by amphipathic aromatic residues that have specific affinity for polar−hydrophobic membrane interfaces. We previously showed that Trp-209, near the cytoplasmic end of TM2, helps maintain the normal baseline-signaling state of the aspartate chemoreceptor (Tar) and that Tyr-210 plays an auxiliary role in this control. We have now repositioned the Trp-209/Tyr-210 pair in single-residue increments about the cytoplasmic polar−hydrophobic interface. Changes from WY−2 to WY+1 modulate the baseline-signaling state of the receptor in predictable and incremental steps that can be compensated by adaptive methylation/demethylation. Greater displacements, as in WY−3, WY+2, and WY+3, bias the receptor to the off kinase-inhibiting state or the on kinase-stimulating state, respectively, to a degree that cannot be fully compensated by the adaptation system. Aromatic residues analogous to Trp-209/Tyr-210 are present in other chemoreceptors and many transmembrane sensor kinases, where they may serve a similar function.

Escherichia coli cells migrate in chemical gradients using a behavior known as chemotaxis. In a homogeneous environment, cells perform a 3D random walk in which smooth swims (runs) of several seconds alternate with briefer periods of active, random reorientation (tumbles). Movement in the gradient is accomplished by selectively increasing the length of runs that happen to lead in a favorable direction, whether up an attractant gradient or down a repellent gradient (*1*). The signal-transduction pathway modulates flagellar motion to increase intervals of exclusively counter-clockwise (CCW[1]) rotation, which produces runs, when the bacterium senses an increase in attractant or a decrease in repellent over time. Thus, a spatial gradient is sensed by temporal comparison of chemoeffector concentrations.

The histidine protein kinase CheA is coupled, via the CheW adapter protein, to four different methyl-accepting chemotaxis proteins, known as MCPs (*2*), and to the Aer redox sensor (*3*, *4*). A receptor/CheA/CheW ternary complex (*5*) stimulates CheA autophosphorylation (*6*). The phosphoryl group on CheA is then transferred to the response regulator CheY. Phospho-CheY interacts with FliM of the flagellar motor to promote clockwise (CW) rotation (*7*, *8*).

CCW motor rotation coalesces the left-handed helical flagellar filaments into a bundle that propels the cell in a run (*9*), whereas CW rotation of one or more flagella disrupts the bundle to cause a tumble (*10*). The intracellular level of phospho-CheY, and hence the frequency of tumbling, is determined by the relative activities of CheA and the phospho-CheY phosphatase, CheZ (*11*, *12*). The conformational change induced by attractant binding converts a receptor from a stimulator (50−100× increase) of CheA activity into an inhibitor (5× decrease) of CheA (*13*). The resulting drop in the intracellular phospho-CheY level lowers the probability of tumbling and thereby lengthens the average run.

Inhibition of CheA activity is balanced by covalent methylation of the cognate receptor (*14*). Methyl groups are added by a methyltransferase, CheR, and removed by CheB, a methylesterase (*15*, *16*). CheB is active when phosphorylated by CheA (*17*). Increased methylation of four specific Glu residues biases a receptor toward CheA stimulation, whereas decreased methylation results in less CheA stimulation (*18*, *19*). By constantly adjusting the extent of methylation, a cell can maintain nearly the same baseline level of CheA activity at any constant concentration of chemoeffector (*20*), and adaptation is robust (*21*).

Tar is the aspartate/maltose chemoreceptor in *E. coli* (*22*). The crystal structure of the periplasmic ligand-binding domains of *Salmonella* (*23*, *24*) and *E. coli* (*25*) Tar show that each monomeric unit of the functional homodimer (*26*, *27*) consists of four antiparallel α-helices in a four-helix

† This work was supported by a grant from the National Institutes of Health (Grant GM39736 to M.D.M.).

* Corresponding author: Tel: (979) 845-5158. Fax: (979) 845-2981. E-mail: mike@mail.bio.tamu.edu.

‡ Present Address: Lark Technologies, Houston, Texas 77099.

[1] Abbreviations: TM1, first transmembrane helix; TM2, second transmembrane helix; CW, clockwise; CCW, counterclockwise; MCP, methyl-accepting chemotaxis protein; H1, periplasmic helix one; H4, periplasmic helix four; HAMP, domain for histidine kinases, adenylyl cyclases, methyl-binding proteins and phosphatases; WALP peptide, tryptophan-flanked poly-(Ala-Leu) peptide; YALP peptide, tyrosine-flanked poly-(Ala-Leu) peptide; Tris, Tris(hydroxymethyl)aminomethane; EDTA, ethylenediaminetetraacetic acid; DTT, dithiothreitol; TCA, trichloroacetic acid; SDS−PAGE, sodium dodecyl sulfate-polyacrylamide gel electrophoresis; ATP, adenosine triphosphate; MRF, mean reversal frequency; NMR, nuclear magnetic resonance.

10.1021/bi061259i CCC: $33.50
Published on Web 11/16/2006

bundle. The first and second transmembrane regions (TM1 and TM2) flanking the periplasmic domain are *N*-terminal and *C*-terminal, respectively, helical extensions of the first (H1) and fourth (H4) periplasmic helices (*28*−*31*). Aspartate binds at one of two rotationally symmetric sites composed of residues in H1 and H4 of one monomer and in H1′ of the other (*24*). Binding generates a 1 to 2 Å vertical displacement of H4-TM2 toward the cytoplasm (*32*−*37*). Within the HAMP-linker domain (*38*, *39*), this piston-like movement is converted into a conformational change in the cytoplasmic domain of the receptor.

TM2 possesses an aliphatic core bracketed by aromatic residues at the polar−hydrophobic interfaces, and positively charged residues reside at the membrane−water interface (*36*). A similar distribution of hydrophobicity, aromaticity, and charge density is often found in membrane-spanning α helices (*40*). Several experimental systems have demonstrated the energetic advantage for the localization of amphipathic aromatic residues at the polar−hydrophobic interfaces. A glycosylation-mapping technique (*41*) implicated Trp residues in positioning a poly-Leu helix within a biological membrane. When the Trp residues were moved, the helix repositioned to allow the Trp residues to remain at the interfacial zone of the membrane (*42*). Also, WALP (*43*) and YALP (*44*) peptides consisting of Ala-Leu cores of different lengths flanked by Trp or Tyr residues, respectively, induce phase transitions in various lipid systems that allow the aromatic residues to reside at polar−hydrophobic interfaces. Thus, amphipathic aromatic residues govern how transmembrane helices interact with their lipid environments.

The position of TM2 relative to the membrane is a critical component of transmembrane signaling. Therefore, interactions between TM2 and the phospholipid bilayer are likely to contribute to the baseline-signaling state of a receptor. Arginine-scanning mutagenesis of *Salmonella* Tar revealed the importance of aromatic residues within TM2. Substitution of Phe-189 or Trp-192 stabilized the kinase-stimulating on state of Tar, whereas substitution of Trp-209 promoted the kinase-inhibiting off state (*36*). We previously demonstrated that Trp-209 is essential for maintaining the normal baseline-signaling state of *E. coli* Tar. Substitution of Ala for Trp-209 puts the mutant receptor into the kinase-inhibiting state typically associated with the binding of aspartate. Tyr-210 also contributes to the positioning of TM2 within the lipid bilayer (*37*). These prior studies identified residues participating in essential membrane−protein interactions that position TM2 within the membrane. Here, we extend these initial analyses by moving the Trp-209/Tyr-210 pair in single-residue increments three positions toward the *N*-terminus (WY−3) and three positions toward the *C*-terminus (WY+3). We demonstrate that, within the context of an intact chemotactic circuit, moving the Trp/Tyr pair tunes the signaling state of Tar in predictable and incremental steps.

MATERIALS AND METHODS

Bacterial Strains and Plasmids. Strains HCB436 (Δ*tsr7021* Δ*trg(100) zbd::Tn5* Δ(*tar-cheB)2234*) (*45*), RP3098 (Δ(*flhD-flhB)4*) (*46*), and VB13 (Δ*tsr7021* Δ*tar-tap5201 trg*::Tn*10*) (*47*) are derivates of the *E. coli* K12 strain RP437 (*48*). Plasmid pRD100 (*37*), derived from pBAD18 (*49*), carries a wild-type copy of *tar* inducible upon the addition of L-arabinose. Plasmid pRD200 (*37*), derived from pMK113 (*50*), harbors a version of the *tar* gene that encodes wild-type Tar attached to a *C*-terminal in-frame sequence for a seven-residue flexible linker and a V5-epitope tag. The *tar* gene of pRD200 is expressed from the native *tar* promoter. Plasmid pRD300 is identical to pRD100 except for the addition of the *C*-terminal linker and the V5-epitope tag from pRD200. Mutations were introduced into *tar* using standard site-directed mutagenesis techniques (Stratagene).

Observation of Tethered Cells. Cells were grown in tryptone broth (*51*) supplemented with 25 μg/mL ampicillin to an $OD_{590\ nm}$ of 0.7. Ten milliliters of cells were resuspended in tethering buffer (10 mM potassium phosphate (pH 7.0), 100 mM NaCl, 10 μM EDTA, 20 μM L-methionine, 20 mM sodium DL-lactate, and 20 μg/mL chloramphenicol), and their flagella were sheared in the 50-mL stainless-steel cup of a Waring blender (*52*). Sheared cells were washed twice in tethering buffer and mixed with an equal volume of a 500-fold dilution of anti-flagellar filament antibody. This mixture was placed inside an Apiezon-L grease ring on a 12 mm round coverslip, incubated for 30 min at 30 °C, and then affixed to a flow chamber (*53*). Tethered cells were observed at 1000× magnification by oil-immersion, reverse-phase contrast microscopy. Enough fields of view were videotaped to ensure that at least 100 freely rotating cells were monitored for each strain in two duplicate experiments. Rotational behavior was visually assessed during video playback, and cells were assigned to one of five rotational categories; exclusively CCW; mostly CCW with occasional reversals; reversing frequently with no clear bias; mostly CW with reversals; and exclusively CW. Reversal frequency was determined by tallying the number of reversals for each cell during video playback.

Determination of the Methylation State of Receptors in Vivo. Cells were grown to an $OD_{590\ nm}$ of 0.6 in 10 mL of tryptone broth (*51*), harvested by centrifugation, washed three times with 10 mM potassium phosphate (pH 7.0) containing 0.1 mM EDTA, and resuspended in 5 mL of 10 mM potassium phosphate (pH 7.0), 10 mM sodium DL-lactate, and 200 μg/mL chloramphenicol. One milliliter aliquots of cells were transferred to 10-mL scintillation vials and incubated with shaking for 10 min at 32 °C. Cells were then incubated for another 30 min after the addition of L-methionine to 2 μM. Chemoeffectors were added at this time, and the cells were incubated for an additional 20 min. Reactions were terminated by the addition of 100 μL of ice-cold 100% TCA and then incubated on ice for 15 min. Denatured proteins were pelleted, subsequently washed with 1% TCA and acetone, and resuspended in 200 μL of 2X SDS-loading buffer. A 10-μL aliquot of each sample was subjected to SDS−PAGE, immunoblotting, and detection by commercially available antibodies raised against the V5 epitope (Invitrogen).

Protein Expression and Isolation. We isolated receptor-containing inner membranes as previously described (*54*). Strain RP3098 harboring pRD100 or one of its derivatives was used for production of receptor-containing membranes. Tar expression was induced by the addition of L-arabinose to a final concentration of 0.2% (w/v). Soluble Che proteins were isolated as previously described (*54*).

Analysis of Receptor Function in Vitro. We performed the receptor-coupled *in vitro* phosphorylation assay as previously described (*37*). Our reactions contained 20 pmol Tar, 5 pmol CheA, 20 pmol CheW, and 500 pmol CheY in 9 μL of fresh phosphorylation buffer (50 mM Tris-HCl, 50 mM KCl, 5 mM $MgCl_2$, and 2 mM DTT (pH 7.5)). Aspartate was added to the desired final concentration, taking care to maintain the same total volume. The reaction was initiated by the addition of 1 μL of [γ-^{32}P]-ATP (3000 Ci/mmol NEN# BLU502A) diluted 1:1 with 10 mM unlabeled ATP. Reactions were terminated by adding 40 μL of 2× SDS−PAGE loading buffer containing 25 mM EDTA. Samples were subjected to SDS−PAGE, dried, and imaged using a phosphorimager (Fuji BAS 5000).

Chemotactic Swarm Assays. Swarm assays were performed as described previously (*37*). Briefly, semisolid agar contained 3.25 g/L Difco BactoAgar in motility medium (10 mM potassium phosphate (pH 7.0), 1 mM $(NH_4)_2SO_4$, 1 mM $MgSO_4$, 1 mM $MgCl_2$, 1 mM glycerol, and 90 mM NaCl) supplemented with 20 μg/mL L-threonine, L-histidine, L-methionine, and L-leucine and 1 μg/mL thiamine. Ampicillin was present at 25 μg/mL. Aspartate and maltose were added to a final concentration of 100 μM. Swarm plates were incubated at 30 °C, and once visible swarms formed, their diameter was measured every 4 h.

RESULTS

Repositioning Trp-209/Tyr-210 of TM2 Relative to the Polar−Hydrophobic Membrane Interface. We have shown that Trp-209 is essential for maintaining the normal baseline-signaling state of Tar and suggested that Tyr-210 plays an auxiliary role in this control (*37*). Inspired by these results and the demonstrated affinity of amphipathic aromatic residues for the polar−hydrophobic interfaces of phospholipid bilayers (*40*, *42*−*44*), we hypothesized that the signaling state of Tar could be modulated by repositioning the tandem residue pair Trp-209/Tyr-210, which localizes to the polar−hydrophobic interface at the cytoplasmic side of the cell membrane (*36*). We used site-directed mutagenesis to construct receptors in which the Trp/Tyr pair was repositioned in single-residue increments from three residues *N*-terminal of their original position (WY−3) to three residues *C*-terminal (WY+3) (Figure 1).

Flagellar Rotation and Reversal Frequency Correlate with the Position of the Trp/Tyr Pair. We tested the hypothesis that repositioning Trp-209/Tyr-210 would result in a displacement of TM2 relative to the membrane and a concomitant change in the baseline-signaling state of the receptor (Figure 1). Rotational bias and reversal frequency in the absence of chemoeffectors were measured in transducer-depleted (ΔT) tethered cells (strain VB13; *47*) expressing the WY−3 through WY+3 Tar receptors from plasmid pRD200. Expression from pRD200 results in a 5-fold excess of total cellular receptor (data not shown). These cells possess an intact chemotactic circuit, and therefore, their behavior should reflect steady-state signaling, which is affected by changes in both the position of TM2 relative to the membrane and the compensatory effects of adaptive methylation (*37*). Approximately 200 cells were analyzed for each receptor variant (Figure 2). Most cells producing wild-type Tar reversed frequently and showed the same CW/CCW bias

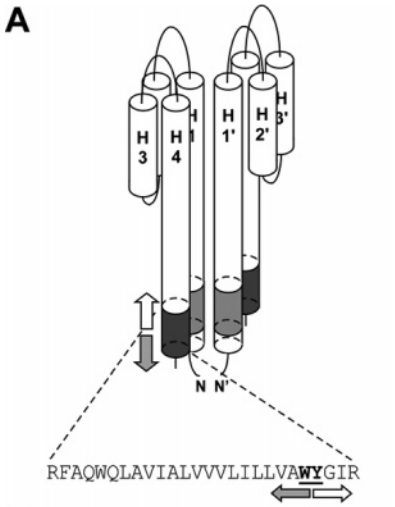

FIGURE 1: Schematic representation of the periplasmic and transmembrane (TM) domains of the wild-type and mutant *E. coli* Tar proteins. (A) TM1 and TM2 are represented as gray- and black-shaded areas, respectively. Aspartate binding displaces TM2 toward the cytoplasm, thereby repositioning TM2 relative to the plane of the phospholipid bilayer (downward gray arrow). Repellent binding displaces TM2 away from the cytoplasm (white upward arrow). The extent of TM2 is based on sulfhydryl-reactivity studies of *S. enterica* Tar (*36*) and includes the Trp-209 and Tyr-210 residues (boldface). (B) Primary sequences of TM2 of the full range of Tar proteins investigated in this study. The Trp/Tyr residue pair is indicated in boldface. The conserved Pro residue of P-type HAMP-linker domains (*39*) provides a reference for the beginning of AS1. The gray, leftward-pointing arrow indicates shifts of the Trp/Tyr pair in the *N*-terminal (−) direction. The white, rightward-facing arrow indicates shifts of the Trp/Tyr pair in the *C*-terminal (+) direction.

(between 20/80 and 40/60%) previously observed with the wild-type strain RP437. A few cells reversed less frequently and were more strongly CW or CCW biased, and a very small number of cells were observed to rotate exclusively in one direction or the other.

Flagella of cells harboring Tar WY−1 or Tar WY−2 exhibited a slight CCW rotational bias compared to those expressing wild-type Tar, and cells expressing WY−3 Tar were even more CCW biased. A CCW bias indicates that these cells had a decreased intracellular concentration of phospho-CheY (*12*), a result consistent with decreased stimulation of CheA by a receptor bearing a displacement of TM2 toward the cytoplasm (*32*). Cells expressing Tar WY+1 were very similar to cells producing the wild-type receptor. WY+2 and WY+3 Tar cells exhibited a bimodal distribution; the majority were CW biased, but some cells were observed whose flagella rotated exclusively CCW. A CW bias is characteristic of increased intracellular levels of phospho-CheY (*12*) and is consistent with the expectation that the displacement of TM2 toward the periplasm should increase the ability of a receptor to stimulate CheA activity.

The mean reversal frequency (MRF) was approximately 0.4 s^{-1} for cells expressing WY−2, WY−1, wild-type, and

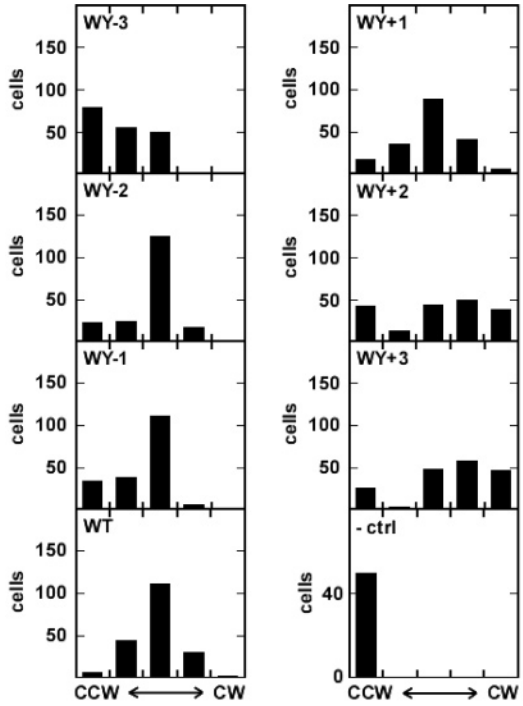

FIGURE 2: Rotational bias of flagella on cells expressing wild-type or mutant Tar proteins. Transducer-depleted VB13 (*cheR*$^+$*B*$^+$) cells expressing the wild-type or mutant Tar proteins from plasmid pRD200 were tethered, observed for 30 s, and placed into one of five categories based on the CW/CCW rotational behavior of their flagella. The five categories of rotation, from left to right, are exclusively CCW; mostly CCW with occasional reversals; reversing frequently with no clear bias; mostly CW with reversals; and exclusively CW. Control (ctrl) cells (bottom right) contained only the empty vector plasmid. Two sets of 100 cells were analyzed for each strain.

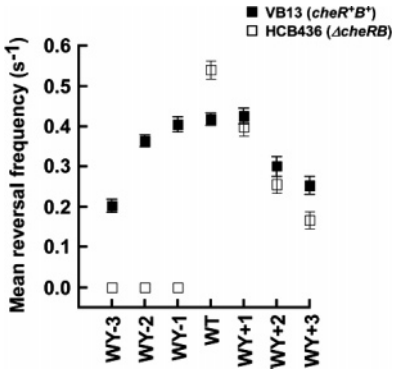

FIGURE 3: Mean reversal frequency (MRF) of the flagella on cells expressing the wild-type or mutant Tar proteins. The same 200 VB13 cells (*cheR*$^+$*B*$^+$) analyzed in Figure 2 (■) and 200 HCB436 cells (Δ*cheRB*) (□) expressing each wild-type or mutant Tar protein from the plasmid pRD200 were tethered as described in Figure 2. Cells were monitored for 30 s, and the number of reversals was determined. Each data point represents the mean number of reversals per second. The error bars represent the standard deviation of the mean, with $n = 200$.

WY+1 Tar. Cells expressing WY−3 Tar had an MRF of 0.2 s^{-1}, whereas cells expressing WY+2 and WY+3 Tar had an MRF of 0.25 s^{-1} (Figure 3). We conclude that cells expressing WY−3, WY+2, and WY+3 Tar have reduced MRF values because the signaling state of these receptors is perturbed to an extent that cannot be entirely compensated by adaptive methylation.

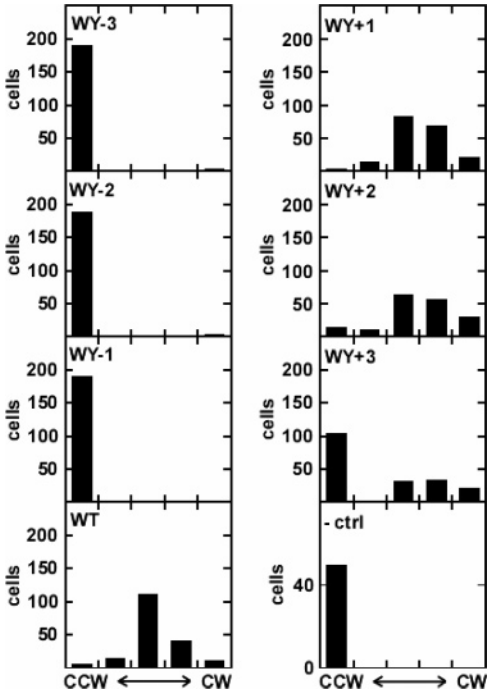

FIGURE 4: Changes in flagellar rotation seen upon repositioning Trp-209/Tyr-210 in the absence of adaptive methylation. The same 200 HCB436 cells (Δ*cheRB*) of each strain for which MRF values were determined (Figure 3) were analyzed as in Figure 2.

Cells Lacking Adaptive Methylation Cannot Compensate for TM2 Displacements. To assess the contribution of adaptive methylation to the signaling state of Tar, we analyzed flagellar rotation in strain HCB436 (ΔT Δ*cheRB*) (*45*). HCB436 cells expressing wild-type Tar displayed a slight CW bias (Figure 4) and high MRF values (∼0.55 s^{-1}) (Figure 3). HCB436 cells producing the WY−3 through WY−1 receptors seldom, if ever, rotated CW (Figure 4). These cells clearly had lower levels of intracellular phospho-CheY than VB13 (ΔT *cheR*$^+$*B*$^+$) cells expressing the equivalent mutant receptors. This finding is consistent with our previous discovery (*37*) that methylation can compensate for an inherently decreased baseline-signaling state of a receptor. The WY+1 protein conferred a modest CW bias to HCB436 cells. Cells producing WY+2 and WY+3 were also CW biased relative to cells expressing wild-type Tar, but a significant number of cells rotated their flagella only CCW. Such cells were also seen when the WY+2 and WY+3 proteins were expressed in strain VB13 (Figure 2), although the fraction of CCW-only cells was lower.

Methylation of Mutant Receptors in Vivo. To demonstrate that methylation restores a more normal baseline-signaling state for the mutant receptors, we analyzed methylation *in vivo*. To create standards for comparison, we expressed the all Gln (QQQQ), all Glu (EEEE), and wild-type (QEQE) forms of Tar in strain RP3098 (Δ*flhD-flhB*) (*46*). During SDS−PAGE, the QQQQ form migrates fastest, the EEEE form slowest, and the QEQE form at an intermediate rate (Figure 5).

WY−1 and WY−2 exhibited increased levels of methylation *in vivo* that were apparently adequate to compensate completely for the inherent CCW bias associated with those receptors in the absence of adaptive methylation (compare Figures 2 and 4). WY−3 Tar had equivalently elevated levels of methylation, but in this case only partial compensation

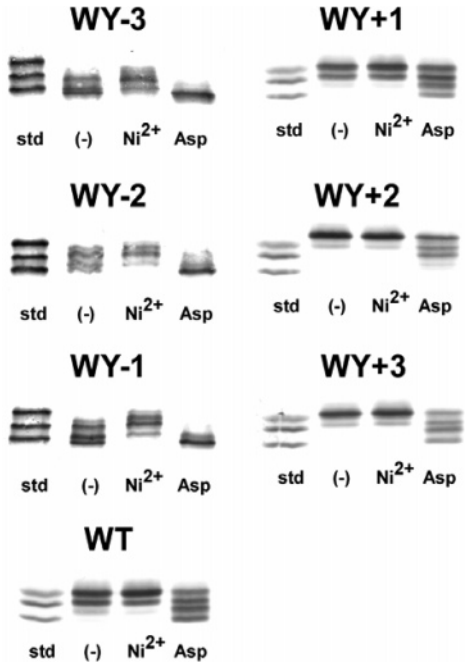

FIGURE 5: Extent of the methylation of mutant Tar proteins *in vivo*. Transducer-depleted VB13 cells expressing the wild-type or mutant Tar proteins from the plasmid pRD200 were exposed to 100 mM aspartate or 10 mM Ni^{2+}. The level of methylation affects the migration rate during SDS−PAGE, with the more highly methylated forms moving faster. As migration standards, the EEEE, QEQE, and QQQQ forms of wild-type Tar were loaded in the leftmost lane. The QEQE and QQQQ forms of Tar migrate like the doubly methylated and quadruply methylated Tar, respectively.

for the inherent CCW bias (Figure 2) associated with the mutant receptor was seen.

In contrast, WY+1 Tar had a very slight decrease in its methylation level compared to wild-type Tar, a finding consistent with the wild-type rotational bias of VB13 cells containing this protein. The methylation level observed with WY+2 and WY+3 Tar was significantly decreased relative to that of the wild-type, but the CW bias of VB13 cells expressing either of those proteins demonstrated that adaptive demethylation cannot completely offset the inherent CW bias imposed by those two receptors.

Apparently, none of the mutant receptors were locked in one conformation. The WY−3 to WY−1 receptors all showed increases in methylation in response to the addition of 100 mM aspartate (Figure 5), although the change with the WY−3 protein was slight. Similarly, all of these receptors became less methylated after the addition of 10 mM Tar-mediated repellent Ni^{2+} (Figure 5). Little change was seen in the methylation state of the wild-type or WY+1, WY+2, and WY+3 proteins in response to Ni^{2+}, but all four proteins became substantially more methylated after the addition of 100 mM aspartate.

Mutant Tar Receptors Possess Reduced Sensitivity to Aspartate. On the basis of the results described thus far, we proposed that the signaling state of Tar correlates with the position of the Trp-209/Tyr-210 pair at the cytoplasmic polar−hydrophobic interface. Furthermore, the mutant receptors still react to either or both aspartate (attractant) and Ni^{2+} (repellent) (Figure 5). It has been suggested that methylation of MCPs in receptor/CheA/CheW ternary complexes causes adaptation by altering the gain between ligand binding and kinase inhibition without substantially altering ligand affinity or kinase stimulation (*55*). If this is true, receptors producing wild-type rotational phenotypes (Tar WY−2 to Tar WY+1) should exhibit different sensitivities to the ligand in proportion to the extent of methylation required to maintain a wild-type rotational bias.

To test this prediction, we expressed both wild-type and mutant receptors from plasmid pRD200 in VB13 (ΔT) cells and analyzed chemotactic migration in motility agar containing aspartate (Figure 6A), maltose, or glycerol (data not shown). Glycerol is a non-attractant carbon source that allows for analysis of aerotaxis in the absence of any specific Tar chemoeffector. The repositioning of Trp-209/Tyr-210 invariably decreased the migration rate to a degree that correlated with the distance they were moved. This was true even for cells expressing Tar WY−2, Tar WY−1, and Tar WY+1, which possess similar baseline rotational biases (Figure 2) and MRFs (Figure 3). We conclude that when Trp-209/Trp-210 are at their original positions, the receptor possesses a level of methylation that allows optimal sensitivity to a gradient of attractant.

We also examined the ability of the mutant receptors to stimulate CheA in the receptor-coupled *in vitro* phosphorylation assay (*13*, *37*), which is performed in the absence of CheR and CheB. We isolated the inner membranes from RP3098 cells in which Tar was expressed from the plasmid pRD100. All Tar in these membranes should be in the QEQE form in which it is initially translated. Tar constituted between 40 and 60% of the total protein in all of the membrane preparations, demonstrating that all of the mutant proteins are reasonably stable. Receptor/CheA/CheW complexes containing wild-type Tar produced 7.8 ± 1.2 pmol phospho-CheY s^{-1} (Figure 6B). The WY−3 through WY−1 receptors all stimulated CheA to less than 10% of this value, a result consistent with displacement of TM2 toward the cytoplasm and the absence of adaptive methylation. The WY+1 to WY+3 receptors all retained the ability to stimulate CheA. The somewhat reduced activities of WY+2 and WY+3 Tar suggest that the transmembrane, HAMP-linker, and cytoplasmic domains may be out of register, somehow resulting in decreased CheA activity.

We also examined the aspartate-induced inhibition of CheA activity for wild-type and mutant receptors *in vitro*. The multisite Hill equation was used to draw a best-fit curve to the data (Figure 6C). With wild-type-Tar, the aspartate K_i was 7 ± 1 μM, and the Hill coefficient was 1.8 ± 0.1, suggesting positive cooperativity. The WY+1 through WY+3 receptors had aspartate K_i values between 10 and 100 μM. Most strikingly, the Hill coefficients were in the range 0.2 ± 0.1, suggesting that there was a strong negative cooperativity for aspartate inhibition.

Methylation has been suggested to cause adaptation by altering the gain between ligand binding and kinase inhibition without altering ligand affinity or kinase stimulation (*55*). Therefore, we hypothesized that receptors producing similar kinase activities *in vivo* should exhibit different sensitivities to the ligand in proportion to the extent of methylation required to maintain a wild-type rotational bias. Our results support this hypothesis and are consistent with the proposed mechanism of adaptive modification (*55*). VB13 (*cheR*$^+$*B*$^+$) cells expressing Tar WY−2 through WY+1 possess similar rotational biases (Figure 2) and MRFs (Figure 3), suggesting

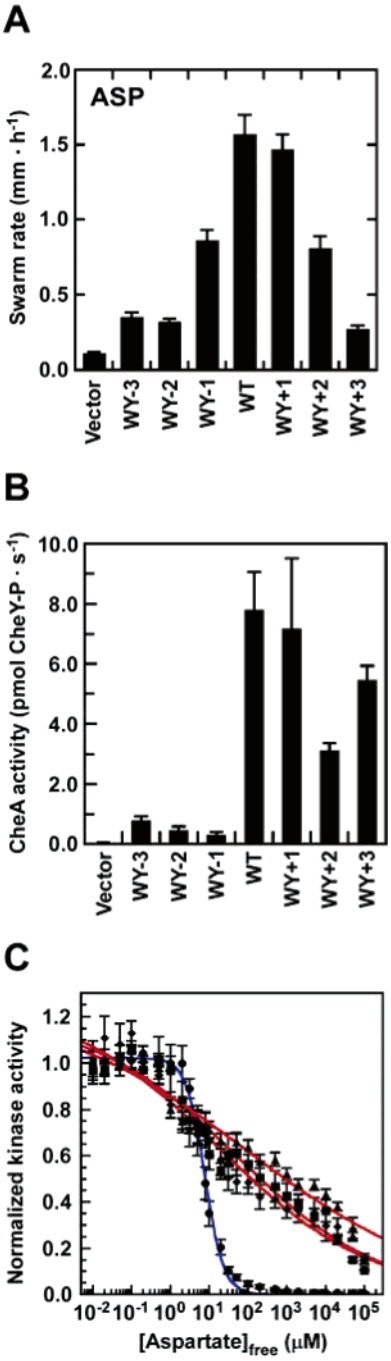

FIGURE 6: Ligand sensitivity of mutant receptors *in vivo* and *in vitro*. (A) The rate at which the swarm diameter increased, measured in mm/h, was analyzed for VB13 cells expressing wild-type or mutant receptors from the plasmid pRD200. The error bars represent the standard deviation, with $n = 3$. (B) CheA kinase-stimulating activity was measured for membranes containing the wild-type and mutant Tar proteins. CheA activities were calculated by averaging the values obtained for at least three independent membrane preparations, each of which was assayed in triplicate. The error bars represent the standard deviation of the mean, with $n = 9$. All receptors were in the QEQE configuration. (C) Aspartate inhibition of receptor-coupled kinase activity of receptor/CheW/CheA complexes containing wild-type (●), WY+1 (■), WY+2 (♦), and WY+3 (▲) Tar proteins. Each data point represents the mean of six total reactions from three independently isolated receptor-containing vesicle preparations. The best-fit curves, represented in blue for the wild-type receptor and red for the mutants, were calculated using the cooperative Hill model. The error bars represent the standard deviation of the mean, with $n = 3$.

similar levels of *in vivo* kinase stimulation. However, these receptors require different levels of methylation to maintain wild-type rotational biases (Figure 5). As hypothesized, we discovered that the sensitivities to a gradient of attractant decreased (Figure 6A) as the extent of methylation (Figure 5) required to maintain wild-type levels of kinase stimulation *in vivo* (Figure 2) increased. In addition, analyses performed in the absence of adaptive modification (Figure 6B and C) support its role in maintaining the relationship between the level of methylation, receptor signaling state, and ligand sensitivity. These observations highlight the enormous restorative power of covalent receptor methylation and underscore the robustness of the adaptation machinery.

DISCUSSION

The binding of aspartate to the periplasmic domain of the Tar chemoreceptor is proposed to displace the second transmembrane helix (TM2), which connects the periplasmic and cytoplasmic domains of the protein, a few ångströms toward the cytoplasm (*32*−*37*). This displacement repositions TM2 relative to the plane of the phospholipid bilayer. Therefore, interactions of TM2 with the membrane may be critical for setting the baseline signaling state of the receptor. Arginine-scanning mutagenesis of *Salmonella* Tar revealed the importance of aromatic residues within TM2. Substitution of Phe-189 or Trp-192 stabilized the on state of Tar, whereas substitution of Trp-209 promoted the off conformation (*36*). We previously showed that Trp-209 and, to a lesser extent, Tyr-210 help maintain the normal baseline-signaling state of *E. coli* Tar (*37*). Here, we extended our previous analysis by systematically moving the Trp-209/Tyr-210 aromatic pair in single-residue steps to precisely modulate the signaling character of Tar. In the context of an intact chemotactic circuit (i.e., in $cheR^+B^+$ cells), this manipulation allows us to tune the signaling properties of Tar in a predictable manner. To our knowledge, this is the first time that protein−membrane interactions have been harnessed to incrementally manipulate the signaling state of a transmembrane receptor over its full range of activities.

A chemoreceptor must process several allosteric inputs, including ligand occupancy, extent of covalent methylation, and higher-order interactions with other chemoreceptors. The frozen dynamic model for modulation of CheA activity (*56*, *57*) suggests that allosteric inputs change the supercoiling state of a four-helix bundle composed of a coiled-coil of two antiparallel helices from each monomer. In the off (attractant-bound) state, the receptor has more conformational freedom, whereas in the on (repellent-bound) state, the four-helix bundle is less dynamic. The adaptation subdomain forms a four-helix bundle that is contiguous with the signaling subdomain (*58*). The four Glu residues that are subject to covalent modification by the CheR methyltransferase may act as an electrostatic switch. Neutralization of the negative charges on these residues, corresponding to methylation *in vivo*, should decrease electrostatic repulsion between the two subunits of a homodimer, resulting in decreased mobility of the signaling domain and increased levels of kinase stimulation (Figure 7A) (*59*, *60*). The HAMP-linker connects TM2 to the adaptation and signaling subdomains. In some fashion, it must transduce vertical displacements of TM2 into changes in helical supercoiling of the cytoplasmic domain.

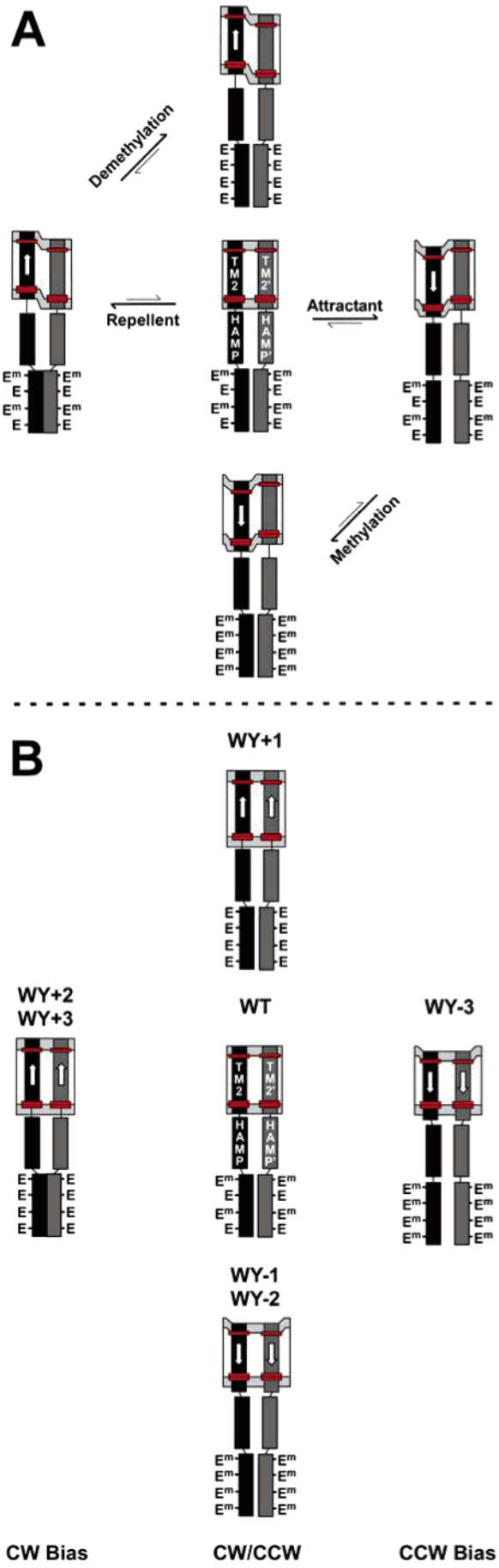

FIGURE 7: Model for how adaptive methylation reverses the signaling biases caused by the displacement of TM2. (A) The frozen dynamic model for modulation of CheA activity (*56*, *57*) suggests that allosteric inputs change the supercoiling state of the signaling subdomain, which forms a contiguous four-helix bundle with the adaptation subdomain (*60*). Neutralization by the methylation of negatively charged Glu residues within the adaptation subdomain decreases electrostatic repulsion between the two subunits of a homodimer, resulting in decreased mobility of the signaling domain and increased levels of kinase stimulation (*59*). This degree of mobility is illustrated as differential spacing between the methylation domains within a Tar homodimer, with a larger spacing indicating higher mobility. In its adapted state, a receptor is in an intermediate signaling state, which leads to CW/CCW flagellar rotation (center). This state may represent equilibrium between fully on (left; exclusively CW flagellar rotation) and fully off (right; exclusively CCW flagellar rotation) states. Attractant binding may displace TM2 into the cytoplasm (right), as indicated by a downward-facing arrow, to produce a localized membrane deformation. The polar regions of the lipid bilayer are represented in dark gray, whereas the hydrophobic core is shown in light gray. The amphipathic aromatic residues near the periplasmic (Trp-192) and cytoplasmic (Trp-209/Tyr-210) ends of TM2 are represented as red boxes. Note that only one TM2 is shown as displaced to account for the asymmetry of attractant-induced signaling (*66*, *67*), although both of the HAMP linkers of the dimer are probably affected, as illustrated. Repellent binding may displace TM2 toward the periplasm as indicated by an upward-facing arrow. For the sake of consistency, repellent signaling is also illustrated as asymmetric, although this has not been experimentally demonstrated. Adaptive methylation and demethylation are envisioned as returning attractant-bound and repellent-bound receptors, respectively, to the intermediate (CW/CCW) signaling state. (B) Repositioning of TM2 by moving the tandem Trp-209/Tyr-210 residues may generate conformational changes similar to those that occur when an attractant or a repellent interacts with the receptor. For relatively small displacements (WY−1 and WY−2, and WY+1), which may correspond to attractant-induced and repellent-induced conformational changes, respectively, the methylation system can compensate to restore nearly normal levels of CheA kinase stimulation *in vivo*. We suggest that repositioning the Trp/Tyr pair produces TM2 displacements that change the distance between the beginning of the HAMP domain and the inner leaflet of the membrane. In the case of the plus series of receptor mutants, the distance decreases (as may happen in response to repellent binding), whereas within the minus series of receptors, this distance would increase (as is thought to happen in response to attractant binding). The displacements of TM2 in WY−3, WY+2, and WY+3 Tar are too large to be completely compensated by adaptive methylation or demethylation. Therefore, these receptors are strongly biased toward the off state (WY−3, right) or the on state (WY+2 and WY+3, left). Note that both TM2s are displaced within the dimer, unlike the asymmetrical displacement of TM2 by attractant or repellent binding as shown in (A).

The steady-state *in vivo* kinase activities, reflected in the rotational biases of tethered cells, associated with the mutant receptors are affected by allosteric contributions from both ligand occupancy and adaptive methylation. Therefore, receptors with different, but still balanced, contributions of ligand binding and adaptive methylation can possess similar activities (Figure 7B). Tar WY−2, Tar WY−1, wild-type Tar, and Tar WY+1 produce similar rotational phenotypes (Figure 2) and mean reversal frequencies (Figure 3) in *cheR*$^+$*B*$^+$ cells, suggesting that they possess equivalent abilities to stimulate CheA *in vivo*. However, each of these receptors is in a different signaling state that reflects changes that are induced by repositioning TM2 and compensated by adaptive methylation (Figure 7B). WY−2 and WY−1 Tar exhibit increased levels of methylation (Figure 5). Conversely, WY+1 is less methylated (Figure 5). Even though

tethered *cheR*$^+$*B*$^+$ cells expressing these mutant receptors have nearly identical CW/CCW ratios of flagellar rotation, the corresponding swimming cells show decreased sensitivity in the chemotaxis swarm assay (Figure 6A).

Methylation of MCPs in receptor/CheA/CheW ternary complexes has been suggested to cause adaptation by altering the gain between ligand binding and kinase inhibition (*55*). Therefore, we predicted that the mutant receptors would possess differences in sensitivity to a gradient of ligand. The results (Figure 6A) support our hypothesis and suggest that when Trp-209/Trp-210 are at their original positions, the receptor possesses a level of methylation *in vivo* that allows optimal sensitivity to a gradient of attractant.

Tar WY−3 possesses the largest displacement of TM2 toward the cytoplasm and produces CCW-biased behavior even in *cheR*$^+$*B*$^+$ tethered cells (Figure 2). In this case, adaptive methylation cannot restore a normal CW/CCW rotational bias. The majority of tethered cells expressing WY+2 and WY+3 Tar exhibit a CW-biased rotational phenotype (Figure 2), suggesting that they also have a displacement of TM2, albeit in the opposite direction, that cannot be fully compensated by demethylation. A subpopulation of *cheR*$^+$*B*$^+$ cells producing these proteins rotate their flagella exclusively CCW, suggesting that in some cells the population of mutant receptors is primarily in an inactive state. Presumably, larger displacements of TM2 toward the periplasm tend to distort Tar into a conformation in which it is unable to stimulate CheA. Our results clearly demonstrate that there are limits to the extent to which TM2 can be repositioned while retaining normal Tar function. The changes conferred by WY−3, WY+2, and WY+3 Tar cannot be compensated by the methylation/demethylation system, suggesting that in these receptors, TM2 is displaced outside its normal range of motion (Figure 7B).

The rotational biases (Figure 4) and mean reversal frequencies (Figure 3) caused by repositioning the Trp/Tyr pair are not graded when the mutant receptors are expressed in Δ*cheRB* cells. The same is true when the mutant receptors are analyzed in the *in vitro* assay for receptor-coupled CheA kinase activity. In the latter assay, the WY−1 through WY−3 receptors all stimulated CheA very weakly (Figure 6B). The WY+1 through WY+3 receptors all stimulated CheA significantly, although Tar WY+2 and WY+3 were considerably less active than wild-type Tar. The most notable difference, however, was in the response to titration by aspartate. The aspartate K_i was somewhat higher for all three mutant proteins, but the biggest difference was in the apparent cooperativity of the inhibition. For wild-type Tar, the apparent Hill coefficient was 1.8, whereas for the WY+1 through WY+3 receptors the apparent Hill coefficient fell to 0.2 (Figure 6C). We do not know whether the increased K_i and decreased cooperativity reflect a lower affinity for aspartate, a partial decoupling of ligand binding and receptor inhibition, or some combination of these effects. The WY−1 to WY−3 receptors, which are inactive in their QEQE forms, may stimulate kinase activity when present in their QQQQ forms, which are equivalent to fully methylated receptors. Conversely, the EEEE forms of WY+1 to WY+3 Tar may exhibit a pattern of aspartate inhibition more like that of QEQE Tar.

Several functional chimeric receptors have been made by fusing the periplasmic, transmembrane, and HAMP-linker domains of chemoreceptors to the signaling domains of sensor kinases (*61*, *62*), and *vice versa* (*52*), suggesting that the mechanism of signal transduction is conserved for these related proteins. Thus, we predict that mutations in transmembrane sensor kinases analogous to the ones described here could generate a graded series of signaling outputs, without the complication of adaptive methylation. Chemoreceptors have also been modified to confer different ligand specificity (*63*, *64*). A combinatorial approach has been used with the bacterial periplasmic binding protein (bPBP) superfamily (*65*) to create chemoreceptors that interact with a broad range of ligands that cannot bind directly to the transmembrane receptors. Modification of any of the allosteric contributions to signaling by such rationally designed proteins, including changes to TM2, the HAMP linker, and the adaptation subdomain, can be used, in principle, to tune their activities.

NOTE ADDED IN PROOF

The solution structure of the HAMP domain of a hyperthermophilic archae was recently determined (*68*) using nuclear magnetic resonance (NMR) spectroscopy. The authors suggest that helical rotations within a parallel coiled-coil domain are responsible for signal propagation. They conclude that their results imply that a piston-type displacement of TM2 cannot be responsible for transmembrane signal transduction (*32*−*37*). Everyone in the field of transmembrane signaling should be excited about the determination of the structure of a soluble HAMP domain. However, the HAMP domain used in this study was hardly typical, which may explain the authors' success in the structural determination of one possible conformation. Furthermore, potential protein−membrane interactions are absent in aqueous solution. We therefore advise caution in drawing sweeping conclusions from this valuable, but necessarily limited, data.

ACKNOWLEDGMENT

Anti-flagellar antibody was a gift from John S. (Sandy) Parkinson (University of Utah, Salt Lake City, UT). Sandy also provided insightful comments and communicated data in advance of publication. We thank the members of the Manson laboratory for beneficial discussions and tireless inspiration. Lilia Z. K. Bartoszek gave the manuscript a final thorough, professional proofreading.

REFERENCES

1. Berg, H. C., and Brown, D. A. (1972) Chemotaxis in *Escherichia coli* analysed by three-dimensional tracking, *Nature 239*, 500−504.
2. Stock, J. B., and Surette, M. G. (1996). Chemotaxis, in *Escherichia coli* and *Salmonella* (Neidardt, F. C. et al., Eds.) pp 1103−1129, ASM Press, Washington, DC.
3. Bibikov, S. I., Biran, R., Rudd, K. E., and Parkinson, J. S. (1997) A signal transducer for aerotaxis in *Escherichia coli*, *J. Bacteriol. 179*, 4075−4079.
4. Rebbapragada, A., Johnson, M. S., Harding, G. P., Zuccarelli, A. J., Fletcher, H. M., Zhulin, I. B., and Taylor, B. L. (1997) The Aer protein and the serine chemoreceptor Tsr independently sense intracellular energy levels and transduce oxygen, redox, and energy signals for *Escherichia coli* behavior, *Proc. Natl. Acad. Sci. U.S.A. 94*, 10541−10546.
5. Francis, N. R., Wolanin, P. M., Stock, J. B., Derosier, D. J., and Thomas, D. R. (2004) Three-dimensional structure and organization of a receptor/signaling complex, *Proc. Natl. Acad. Sci. U.S.A. 101*, 17480−17485.

6. Borkovich, K. A., Kaplan, N., Hess, J. F., and Simon, M. I. (1989) Transmembrane signal transduction in bacterial chemotaxis involves ligand-dependent activation of phosphate group transfer, *Proc. Natl. Acad. Sci .U.S.A. 86*, 1208−1212.
7. Ravid, S., Matsumura, P., and Eisenbach, M. (1986) Restoration of flagellar clockwise rotation in bacterial envelopes by insertion of the chemotaxis protein CheY, *Proc. Natl. Acad. Sci. U.S.A. 83*, 7157−7161.
8. Welch, M., Oosawa, K., Aizawa, S., and Eisenbach, M. (1993) Phosphorylation-dependent binding of a signal molecule to the flagellar switch of bacteria, *Proc. Natl. Acad. Sci. U.S.A. 90*, 8787−8791.
9. Silverman, M., and Simon, M. (1974) Flagellar rotation and the mechanism of bacterial motility, *Nature 249*, 73−74.
10. Turner, L., Ryu, W. S., and Berg, H. C. (2000) Real-time imaging of fluorescent flagellar filaments, *J. Bacteriol. 182*, 2793−2801.
11. Hess, J. F., Oosawa, K., Kaplan, N., and Simon, M. I. (1988) Phosphorylation of three proteins in the signaling pathway of bacterial chemotaxis, *Cell 53*, 79−87.
12. Cluzel, P., Surette, M., and Leibler, S. (2000) An ultrasensitive bacterial motor revealed by monitoring signaling proteins in single cells, *Science 287*, 1652−1655.
13. Borkovich, K. A., and Simon, M. I. (1990) The dynamics of protein phosphorylation in bacterial chemotaxis, *Cell 63*, 1339−1348.
14. Goy, M. F., Springer, M. S., and Adler, J. (1977) Sensory transduction in *Escherichia coli*: role of a protein methylation reaction in sensory adaptation, *Proc. Natl. Acad. Sci. U.S.A. 74*, 4964−4968.
15. Springer, W. R., and Koshland, D. E., Jr. (1977) Identification of a protein methyltransferase as the cheR gene product in the bacterial sensing system, *Proc. Natl. Acad. Sci. U.S.A. 74*, 533−537.
16. Stock, J. B., and Koshland, D. E., Jr. (1978) A protein methylesterase involved in bacterial sensing, *Proc. Natl. Acad. Sci. U.S.A. 75*, 3659−3663.
17. Lupas, A., and Stock, J. (1989) Phosphorylation of an N-terminal regulatory domain activates the CheB methylesterase in bacterial chemotaxis, *J. Biol. Chem. 264*, 17337−17342.
18. Bornhorst, J. A., and Falke, J. J. (2000) Attractant regulation of the aspartate receptor-kinase complex: limited cooperative interactions between receptors and effects of the receptor modification state, *Biochemistry 39*, 9486−9493.
19. Li, G., and Weis, R. M. (2000) Covalent modification regulates ligand binding to receptor complexes in the chemosensory system of *Escherichia coli*, *Cell 100*, 357−365.
20. Goy, M. F., Springer, M. S., and Adler, J. (1978) Failure of sensory adaptation in bacterial mutants that are defective in a protein methylation reaction, *Cell 15*, 1231−1240.
21. Alon, U., Surette, M. G., Barkai, N., and Leibler, S. (1999) Robustness in bacterial chemotaxis, *Nature 397*, 168−171.
22. Springer, M. S., Goy, M. F., and Adler, J. (1977) Sensory transduction in *Escherichia coli*: two complementary pathways of information processing that involve methylated proteins, *Proc. Natl. Acad. Sci. U.S.A. 74*, 3312−3316.
23. Milburn, M. V., Prive, G. G., Milligan, D. L., Scott, W. G., Yeh, J., Jancarik, J., Koshland, D. E., Jr., and Kim, S. H. (1991) Three-dimensional structures of the ligand-binding domain of the bacterial aspartate receptor with and without a ligand, *Science 254*, 1342−1347.
24. Yeh, J. I., Biemann, H. P., Prive, G. G., Pandit, J., Koshland, D. E., Jr., and Kim, S. H. (1996) High-resolution structures of the ligand binding domain of the wild-type bacterial aspartate receptor, *J. Mol. Biol. 262*, 186−201.
25. Bowie, J. U., Pakula, A. A., and Simon, M. I. (1995) The three-dimensional structure of the aspartate receptor from *Escherichia coli*, *Acta. Crystallogr., Sect. D 51*, 145−154.
26. Falke, J. J., and Koshland, D. E., Jr. (1987) Global flexibility in a sensory receptor: a site-directed cross-linking approach, *Science 237*, 1596−1600.
27. Milligan, D. L., and Koshland, D. E., Jr. (1988) Site-directed cross-linking. Establishing the dimeric structure of the aspartate receptor of bacterial chemotaxis, *J. Biol. Chem. 263*, 6268−6275.
28. Lynch, B. A., and Koshland, D. E., Jr. (1991) Disulfide cross-linking studies of the transmembrane regions of the aspartate sensory receptor of *Escherichia coli*, *Proc. Natl. Acad. Sci. U.S.A. 88*, 10402−10406.
29. Pakula, A. A., and Simon, M. I. (1992) Determination of transmembrane protein structure by disulfide cross-linking: the *Escherichia coli* Tar receptor, *Proc. Natl. Acad. Sci. U.S.A. 89*, 4144−4148.
30. Stoddard, B. L., Bui, J. D., and Koshland, D. E., Jr. (1992) Structure and dynamics of transmembrane signaling by the *Escherichia coli* aspartate receptor, *Biochemistry 31*, 11978−11983.
31. Scott, W. G., and Stoddard, B. L. (1994) Transmembrane signalling and the aspartate receptor, *Structure 2*, 877−887.
32. Chervitz, S. A., and Falke, J. J. (1995) Lock on/off disulfides identify the transmembrane signaling helix of the aspartate receptor, *J. Biol. Chem. 270*, 24043−24053.
33. Hughson, A. G., and Hazelbauer, G. L. (1996) Detecting the conformational change of transmembrane signaling in a bacterial chemoreceptor by measuring effects on disulfide cross-linking *in vivo*, *Proc. Natl. Acad. Sci. U.S.A. 93*, 11546−11551.
34. Ottemann, K. M., Xiao, W., Shin, Y. K., and Koshland, D. E., Jr. (1999) A piston model for transmembrane signaling of the aspartate receptor, *Science 285*, 1751−1754.
35. Isaac, B., Gallagher, G. J., Balazs, Y. S., and Thompson, L. K. (2002) Site-directed rotational resonance solid-state NMR distance measurements probe structure and mechanism in the transmembrane domain of the serine bacterial chemoreceptor, *Biochemistry 41*, 3025−3036.
36. Miller, A. S., and Falke, J. J. (2004) Side chains at the membrane−water interface modulate the signaling state of a transmembrane receptor, *Biochemistry 43*, 1763−1770.
37. Draheim, R. R., Bormans, A. F., Lai, R.-Z., and Manson, M. D. (2005) Tryptophan residues flanking the second transmembrane helix (TM2) set the signaling state of the Tar chemoreceptor, *Biochemistry 44*, 1268−1277.
38. Aravind, L., and Ponting, C. P. (1999) The cytoplasmic helical linker domain of receptor histidine kinase and methyl-accepting proteins is common to many prokaryotic signalling proteins, *FEMS Microbiol. Lett. 176*, 111−116.
39. Williams, S. B., and Stewart, V. (1999) Functional similarities among two-component sensors and methyl-accepting chemotaxis proteins suggest a role for linker region amphipathic helices in transmembrane signal transduction, *Mol. Microbiol. 33*, 1093−1102.
40. de Planque, M. R., and Killian, J. A. (2003) Protein-lipid interactions studied with designed transmembrane peptides: role of hydrophobic matching and interfacial anchoring, *Mol. Membr. Biol. 20*, 271−284.
41. Nilsson, I., Saaf, A., Whitley, P., Gafvelin, G., Waller, C., and von Heijne, G. (1998) Proline-induced disruption of a transmembrane alpha-helix in its natural environment, *J. Mol. Biol. 284*, 1165−1175.
42. Braun, P., and von Heijne, G. (1999) The aromatic residues Trp and Phe have different effects on the positioning of a transmembrane helix in the microsomal membrane, *Biochemistry 38*, 9778−9782.
43. Killian, J. A., Salemink, I., de Planque, M. R., Lindblom, G., Koeppe, R. E., II, and Greathouse, D. V. (1996) Induction of nonbilayer structures in diacylphosphatidylcholine model membranes by transmembrane alpha-helical peptides: importance of hydrophobic mismatch and proposed role of tryptophans, *Biochemistry 35*, 1037−1045.
44. de Planque, M. R., Boots, J. W., Rijkers, D. T., Liskamp, R. M., Greathouse, D. V., and Killian, J. A. (2002) The effects of hydrophobic mismatch between phosphatidylcholine bilayers and transmembrane alpha-helical peptides depend on the nature of interfacially exposed aromatic and charged residues, *Biochemistry 41*, 8396−8404.
45. Wolfe, A. J., and Berg, H. C. (1989) Migration of bacteria in semisolid agar, *Proc. Natl. Acad. Sci. U.S.A. 86*, 6973−6977.
46. Smith, R. A., and Parkinson, J. S. (1980) Overlapping genes at the cheA locus of *Escherichia coli*, *Proc. Natl. Acad. Sci. U.S.A. 77*, 5370−5374.
47. Weerasuriya, S., Schneider, B. M., and Manson, M. D. (1998) Chimeric chemoreceptors in *Escherichia coli*: signaling properties of Tar-Tap and Tap-Tar hybrids, *J. Bacteriol. 180*, 914−920.
48. Smith, R. A., and Parkinson, J. S. (1980) Overlapping genes at the cheA locus of *Escherichia coli*, *Proc. Natl. Acad. Sci. U.S.A. 77*, 5370−5374.

49. Guzman, L. M., Belin, D., Carson, M. J., and Beckwith, J. (1995) Tight regulation, modulation, and high-level expression by vectors containing the arabinose PBAD promoter, *J. Bacteriol. 177*, 4121−4130.
50. Gardina, P., Conway, C., Kossman, M., and Manson, M. (1992) Aspartate and maltose-binding protein interact with adjacent sites in the Tar chemotactic signal transducer of *Escherichia coli*, *J. Bacteriol. 174*, 1528−1536.
51. Miller, J. H. (1972) *Experiments in Molecular Genetics*, Cold Spring Harbor Laboratory, Cold Spring Harbor, NY.
52. Ward, S. M., Bormans, A. F., and Manson, M. D. (2006) Mutationally altered signal output in the Nart (NarX-Tar) hybrid chemoreceptor, *J. Bacteriol. 188*, 3944−3951.
53. Berg, H. C., and Block, S. M. (1984) A miniature flow cell designed for rapid exchange of media under high-power microscope objectives, *J. Gen. Microbiol. 130*, 2915−2920.
54. Lai, R.-Z., Manson, J. M., Bormans, A. F., Draheim, R. R., Nguyen, N. T., and Manson, M. D. (2005) Cooperative signaling among bacterial chemoreceptors, *Biochemistry 44*, 14298−14307.
55. Levit, M. N., and Stock, J. B. (2002) Receptor methylation controls the magnitude of stimulus-response coupling in bacterial chemotaxis, *J. Biol. Chem. 277*, 36760−36765.
56. Kim, S. H. (1994) "Frozen" dynamic dimer model for transmembrane signaling in bacterial chemotaxis receptors, *Protein Sci. 3*, 159−165.
57. Kim, S. H., Wang, W., and Kim, K. K. (2002) Dynamic and clustering model of bacterial chemotaxis receptors: structural basis for signaling and high sensitivity, *Proc. Natl. Acad. Sci. U.S.A. 99*, 11611−11615.
58. Bass, R. B., and Falke, J. J. (1998) Detection of a conserved alpha-helix in the kinase-docking region of the aspartate receptor by cysteine and disulfide scanning, *J. Biol. Chem. 273*, 25006−25014.
59. Starrett, D. J., and Falke, J. J. (2005) Adaptation mechanism of the aspartate receptor: electrostatics of the adaptation sub-domain play a key role in modulating kinase activity, *Biochemistry 44*, 1550−1560.
60. Winston, S. E., Mehan, R., and Falke, J. J. (2005) Evidence that the adaptation region of the aspartate receptor is a dynamic four-helix bundle: cysteine and disulfide scanning studies, *Biochemistry 44*, 12655−12666.
61. Utsumi, R., Brissette, R. E., Rampersaud, A., Forst, S. A., Oosawa, K., and Inouye, M. (1989) Activation of bacterial porin gene expression by a chimeric signal transducer in response to aspartate, *Science 245*, 1246−1249.
62. Baumgartner, J. W., Kim, C., Brissette, R. E., Inouye, M., Park, C., and Hazelbauer, G. L. (1994) Transmembrane signalling by a hybrid protein: communication from the domain of chemoreceptor Trg that recognizes sugar-binding proteins to the kinase/phosphatase domain of osmosensor EnvZ, *J. Bacteriol. 176*, 1157−1163.
63. Dwyer, M. A., Looger, L. L., and Hellinga, H. W. (2003) Computational design of a Zn2+ receptor that controls bacterial gene expression, *Proc. Natl. Acad. Sci. U.S.A. 100*, 11255−11260.
64. Derr, P., Boder, E., and Goulian, M. (2006) Changing the specificity of a bacterial chemoreceptor, *J. Mol. Biol. 355*, 923−932.
65. Dwyer, M. A., and Hellinga, H. W. (2004) Periplasmic binding proteins: a versatile superfamily for protein engineering, *Curr. Opin. Struct. Biol. 14*, 495−504.
66. Gardina, P. J., and Manson, M. D. (1996) Attractant signaling by an aspartate chemoreceptor dimer with a single cytoplasmic domain, *Science 274*, 425−426.
67. Tatsuno, I., Homma, M., Oosawa, K., and Kawagishi, I. (1996) Signaling by the *Escherichia coli* aspartate chemoreceptor Tar with a single cytoplasmic domain per dimer, *Science 274*, 423−425.
68. Hulko, M., Berndt, F., Gruber, M., Linder, J. U., Truffault, V., Schultz, A., Martin, J., Schultz, J. E., Lupas, A. N., and Coles. M. (2006) The HAMP domain structure implies helix rotation in transmembrane signaling, *Cell 126*, 929−940.

BI061259I